Excited State Intramolecular Charge Transfer Reaction in Binary Mixtures of Water and Tertiary Butanol (TBA): Alcohol Mole Fraction Dependence

Tuhin Pradhan, Piue Ghoshal, and Ranjit Biswas*

Department of Chemical, Biological and Macromolecular Sciences, and Unit for Nanoscience and Technology, S. N. Bose National Centre for Basic Sciences, JD Block, Sector III, Salt Lake City, Kolkata 700 098, India

Received: September 2, 2007; In Final Form: November 3, 2007

The excited state intramolecular charge transfer reaction of 4-(1-azetidinyl)benzonitrile (P4C) has been studied in water−tertiary butanol (TBA) mixtures at different alcohol mole fractions by using steady state and time-resolved fluorescence spectroscopy. The ratio between the areas under the locally excited (LE) and charge transferred (CT) emission bands is found to exhibit a sharp rise at alcohol mole fraction ∼0.04, a value at which several thermodynamic properties of this mixture is known to show anomalous change due to the enhancement of H-bonding network. The radiative rate associated with the LE emission also shows a maximum at this TBA mole fraction. Although the structural transition from the water-like tetrahedral network to the alcohol-like chain is reflected in the red shift of the absorption spectrum up to TBA mole fraction ∼0.10, the emission bands (both LE and CT) show the typical nonideal alcohol mole fraction dependence at all TBA mole fractions. Quantum yield, CT radiative rate as well as transition moments also exhibit a nonideal alcohol mole fraction dependence. The time-resolved emission decay of P4C has been found to be biexponential at all TBA mole fractions, regardless of emission collection around either the LE or the CT bands. The time constant associated with the slow component (τ_{slow}) shows a minimum at TBA mole fraction ∼0.04, whereas such a minimum for the fast time constant, τ_{fast} (representing the rate of LE → CT conversion reaction) is not observed. The nonobservation of the minimum in τ_{fast} might be due to the limited time resolution employed in our experiments.

I. Introduction

Photoinduced charge transfer reaction in the substituted benzonitrile derivatives has been studied extensively since the discovery of dual fluorescence in 4-*N*,*N*-dimethylaminobenzonitrile (DMABN).[1−17] Photoinduced charge transfer is an important process in biology as light-induced charge separation plays key roles in photosynthesis and vision. The possibility of using molecules undergoing intramolecular charge transfer reaction in optoelectronic devices as molecular switches further fuels the research in this area. Therefore, a thorough understanding of light-induced intramolecular charge transfer reaction in various environments is extremely important not only for basic science relating chemistry and physics but also for biology and technology. Experimental studies in conjunction with semiempirical quantum mechanical calculations have been employed to correlate the experimental data with the energy differences between states in the gas phase.[5,15] Typically, a single emission band characterizes the fluorescence emission spectrum of DMABN and related derivatives in nonpolar solvents.[1−5] However, in polar solvents a new anomalously red-shifted fluorescence emission band appears which is in addition to the normal emission found in nonpolar solvents.[1−5] The appearance of these two emission bands is a reflection of intramolecular charge transfer reaction in the excited state and several models have been proposed to explain the new emission in polar environments. A detailed discussion on these models and experimental results supporting each of the models are recently provided in an elegant review by Grabowski and co-workers.[1] A common feature in all these models is that the new emission in polar solvents is arising from an electronic state of charge transfer (CT) character, whereas the normal fluorescence is from a locally excited (LE) character with charge distribution similar to that in the ground state. Upon photoexcitation, a substantial amount of charge is transferred from the amino group to benzonitrile moiety forming the CT state. Consequently, the more polar CT state would be further stabilized by polar solvent via enhanced dipole−dipole interaction between dipolar solvent molecules and photoexcited solute. According to the twisted intramolecular charge transfer (TICT) model, the charge transfer process occurs with the simultaneous twisting of the bond connecting the amino group and the benzene ring.[1−5] The molecules in which the excited state intramolecular charge transfer reaction can be explained in terms of TICT mechanism are termed as TICT molecules. Further evidence for the TICT mechanism come from the experimentally observed viscosity dependence of the rate of LE → CT conversion reaction and also presence of two distinct species in the photoexcited compounds. Recently, effects of electrolyte on the LE → CT conversion reaction rate have been analyzed[18,19] using the Zwan and Hynes formalism[20] for electrolyte friction experienced by a rotating moiety in a model isomerization reaction. The agreement between theory and experiments found in this study[18,19] also provides further support to the TICT mechanism for the excited state intramolecular charge transfer reaction.

As the LE → CT conversion reaction is facilitated by solvent reorganization and thus dominated by the orientational solvent polarization density relaxation,[21,22] dynamical solvent modes are expected to modify considerably the rate of intramolecular charge transfer reaction in TICT molecules. Recently, Maroncelli

* Corresponding author. E-mail: ranjit@bose.res.in.

10.1021/jp0770460 CCC: $40.75
Published on Web 01/16/2008

and co-workers have explored the solvent control on the LE → CT conversion reaction of several TICT molecules with amino groups in four-, five-, and six-membered rings attached to benzonitrile moiety.[5] These studies have indicated substantial effects of solvent dynamical modes on reaction rates in these molecules. As the LE → CT conversion reaction in these molecules involves low barrier (~5 k_BT),[5] the reaction time scale (given by the inverse of the barrier frequency) lies typically in the picosecond regime.[21] In many complex liquids, particularly in binary mixtures,[23−35] confined liquids,[36] and electrolyte solutions,[37−40] the environmental reorganization occurs at a time scale much slower than this. Because interdiffusion and preferential solvation are responsible for the slow dynamics in binary mixtures,[23−35] these factors can affect the reaction rate by slow stabilization of the product. In addition, the polarity and time scales associated with the dynamics of solution can be continuously changed by varying the mole fraction of one of the components.[23−25] Therefore, solvent effects on the charge transfer reaction are expected to be more complex and can provide rich information regarding the environmental coupling of the TICT reaction in solution phase. Because solvent structure (spatial arrangement) and dynamics are intimately related,[22] the modification in solution structure in the presence of the second component also modulates several equilibrium aspects, such as equilibrium constant (K_{eq}), change in reaction free energy (ΔG_r), and the peak positions of spectral bands and their bandwidths. Enhancement of structure or weakening of it may affect both the reaction rate and product of a TICT reaction because better packing induces increased solvation of both reactants and products. Also, this will induce red shift of the absorption and emission spectra of a polarity probe dissolved in such media.

In the work presented here, alcohol mole fraction dependence of TICT reaction in water−tertiary butanol (water−TBA) system has been studied. Because the miscibility of alcohols decreases with increase in the size of alkyl residue, TBA is the largest alcohol that remains fully miscible with water at all proportions.[41−44] Consequently, it shows the maximum hydrophobic effects among the short-chain water-soluble alcohols. Interestingly, hydrophobic hydration and its effects are known to play crucial roles in determining functions of many biologically relevant macromolecules and hence an understanding of hydrophobic effects is particularly necessary.[45,46] This is probably one of the reasons that drives much of the efforts to understand the solution structure of alcohol−water systems in general and water−TBA mixtures in particular. Neutron diffraction studies of water−TBA systems indicate addition of water modifies the H-bonding interactions in the mixture which, in turn, facilitates the hydrophobic interactions between the tertiary butyl groups of the TBA molecules.[47−49] This hydrophobic interaction drives the association of TBA molecules by bringing in the alkyl groups closer to each other at all TBA concentrations. This leads to the microscopic heterogeneity in solution which is found to be rather generic in nature for water−alcohol systems.[50,51] In addition, these studies suggest that clathrate-like water−TBA complex may not exist even at low TBA concentrations even though the basic tetrahedral motif of short-range intermolecular water structure is preserved in both dilute and concentrated alcohol−water solutions. According to these studies, water molecules exist as small H-bonded strings or clusters in a fluid of close-packed alkyl groups where water−alcohol H-bonding replaces the alcohol−alcohol H-bonding.[50,51] Light scattering,[52,53] small-angle X-ray scattering,[54−56] dielectric relaxation,[57,58] Raman spectroscopy,[59,60] and several computer simulation[61,62] and numerical[63−65] studies seem to suggest the strengthening of water structure upon small addition of alcohol molecules which is gradually transformed to zigzag alcohol-like structure as the alcohol concentration is increased. All these studies, however, point out that incomplete mixing between the water and alcohol molecules at the molecular level and the retention of three-dimensional H-bonding network structure of water might be responsible for the observed anomalous behavior of thermodynamics properties in aqueous solutions at low alcohol concentrations.

Because microscopic phase separation is inherent in TBA−water mixtures,[47−65] TICT reaction in TBA−water solutions are expected to be affected by such heterogeneity in solution structure. However, the micro-heterogeneity may be less pronounced in presence of a TICT molecule as a recent neutron diffraction study with ternary mixture composed of cyclohexene, TBA, and water in a 2:6:1 ratio indicate that the nonpolar cyclohexene molecules are favorably solvated by the alkyl groups of the alcohol molecules where the trimolecular mixture appears to be more homogeneous than the binary TBA−water solutions.[49] Several studies have been done earlier with DMABN in alcohol−alkane mixtures where formation of alcohol−DMABN exciplex was believed to play key roles in regulating the CT emission decay.[16,66−68] Effects of structural modification upon the addition of alkane have not been stressed in these studies. Such a study with 4-(1-azetidinyl)benzonitrile (P4C) in water−TBA mixtures at different alcohol mole fractions are presented here for the first time to the best of our knowledge.

As the TICT reaction in P4C is investigated in aqueous solutions of TBA at different concentrations, one would like to ask the following questions. First, will the strengthening of water structure due to addition of alcohol at low concentration and the resultant heterogeneity be reflected as the TICT reaction is carried out at different mole fractions? More precisely, can the TICT reaction be used as a probe to investigate the sharp change in solution structure[41−44] that occurs at the water rich regime with a peak at TBA mole fractions ~0.04? This is possible only when the local solution structure is strongly coupled to the mechanism of TICT reaction, even though the usual nonideality of solution polarity is expected to affect the reaction accordingly. Second, will the equilibrium ground state solvation (as probed by the steady state absorption) be different from that of excited state (as probed by the steady state fluorescence emission)? Note that simulation studies[61] have indicated that the average lifetime of the TBA clusters is in the range 20−30 ps, which is much shorter than the average fluorescence lifetime of either LE or CT states. Therefore, many fluctuations in the environment surrounding the excited probe molecule may obscure the signature of each of the specific environments, leading to the emission from an "averaged-out" environment.[23] In such cases, the stronger solute−solvent dipolar interaction is the only factor that drives the solvent rearrangement around the photoexcited solute and the fluorescence emission will reflect the average nonideality in solution polarity of alcohol−water binary mixtures. Third, what would be the effects of such solution structural change on the rate of intramolecular charge transfer reaction occurring in TBA−water solutions? Fourth, what would be the effects of mole fraction dependent solution dynamics on TICT reaction occurring in TBA−water solutions?

In this article we present the results on the excited state intramolecular charge transfer reaction of 4-(1-azetidinyl)-benzonitrile (P4C) in aqueous TBA solutions at several alcohol mole fractions where we have investigated some of the questions posed above. We use the TICT model to analyze our data as done earlier for studies in pure solvents[5] and electrolyte

solutions.[18−19] We assume that the reaction is in the rapid equilibration limit and hence a biexponential decay of intensity with time is expected.[5,18−19] The assumption of the rapid equilibration limit becomes inappropriate if solution dynamics becomes considerably slower. Interestingly, a biexponential function with two different time constants is found to sufficiently describe the decay kinetics of P4C at all TBA concentrations, as has been found earlier in electrolyte solutions.[19]

The main results of this paper are as follows. Quantum yields, transition moments, and radiative and nonradiative rates for P4C molecule have been determined as a function of TBA mole fraction. All these quantities reflect the mole fraction dependent nonideal nature of TBA−water solutions. The peak frequencies of both the LE and CT emission bands of P4C also show the similar nonideal TBA mole fraction dependence. This is strikingly different from the alcohol mole fraction dependence of the P4C absorption spectrum where the absorption peak frequency shifts initially toward red with TBA concentration (up to ∼0.1 mole fraction) and then blue shifts with TBA mole fraction in a manner similar to what has been found for emission frequencies. As expected, the frequency shift associated with the CT emission band as a function of TBA mole fraction is larger than those observed for the LE and absorption bands. The ratio between the areas under the LE and CT emission bands (CT/LE) increases initially upon addition of TBA and shows a peak at TBA mole fraction ∼0.04 and then decreases in a fashion that resembles the nonideal TBA mole fraction dependence. The time constant associated with the slower part of the emission decay is found to show a sharp minimum at TBA mole fraction ∼0.04, reflecting the effects of structural enhancement at low alcohol concentration in water−TBA mixtures. Such a minimum is not observed for the faster time constant which may be due to the limited time resolution employed in the present work.

The organization of the rest of the paper is as follows. Experimental details are given in the next section. Section III contains experimental results from our steady state and time dependent studies with P4C molecules in aqueous solution of TBA with different TBA mole fractions. The paper then ends with concluding remarks in section V.

II. Experimental Details

4-(1-Azetidinyl)benzonitrile (P4C) was synthesized by following a protocol given in literature[8] and recrystallized twice from cyclohexane (Merck, Germany). Purity of the compound was then checked by thin layer chromatography and monitoring the excitation wavelength dependence of the fluorescence emission.

Tertiary butyl alcohol (TBA) was obtained from Aldrich and used as received. Deionized water (Millipore) was used for preparing the aqueous solutions of TBA at different mole fractions. The solutions were prepared by dissolving a measured amount of TBA in a 10 mL volumetric flask followed by shaking the solution for a few minutes. Caution was exercised to ensure the accuracy of the mole fraction, particularly near the very low TBA and water concentrations. A fraction of this stock solution was then taken into a quartz cuvette of optical path length 1 cm. Subsequently, a small grain of P4C was dissolved and stirred the solution for ∼10 min and absorption spectrum recorded (Model UV-2450, Shimadzu). Note that the concentration of P4C was maintained at $\leq 10^{-5}$ M in all TBA mole fractions studied here. The emission spectra were recorded (SPEX Fluoromax-3, Jobin-Yvon, Horiba) after adjusting the absorbance of the solution to 0.1 or less with excitation wavelength fixed at 305 nm. Solvent blanks were subtracted from the emission spectra prior to analysis and converted to frequency representation after properly weighting the intensity with λ^2. As bubbling few samples with dry argon gas showed very little or no effects on the average rate, most of the samples were not deoxygenated.[5,18−19]

We then used emission spectrum of P4C in perfluorohexane (reference emission spectrum) to deconvolute each emission spectrum into two fragments.[5] This deconvolution provided areas under LE and CT emission bands that were then used to calculate several spectroscopic quantities. Emission peak frequencies were calculated as follows. Shifts of the emission spectra from the peak of the reference emission spectrum were calculated and then added to the *average* peak frequency of the reference emission spectrum. The *average* peak frequency of the reference spectrum was calculated by simply averaging the numbers obtained by fitting the upper half of the spectrum with an inverted parabola, first moment and the arithmetic mean of the frequencies at half intensities on both blue and red ends of the reference emission spectrum.[69−71] Similar procedure was also used to determine the absorption peak frequencies except that no deconvolution was performed in this case.

Time-resolved fluorescence emission intensity decays were collected using a time correlated single photon counting (TCSPC) technique based on a laser system (Lifespec-ps, Edinburgh, UK) with a light emitting diode (LED) that provided 299 nm light as excitation. The full width at half-maximum of the instrument response function (IRF) with the above excitation was approximately 475 ps. The emission decay was collected at magic angle at both LE and CT peak positions (of steady state spectrum) with an emission band-pass of 8 nm. Subsequently, the collected emission decays were deconvoluted from the IRF and fitted to multiexponential function using an iterative reconvolution algorithm.[5] Such fitting enables one to capture decay kinetics with a time constant as fast as ∼100 ps with reasonable accuracy.[5] For a few cases, emission decays were collected at two or three different emission wavelengths around the LE and CT peaks and the analyzed data were found to vary within a small uncertainty. All the experiments were performed at room temperature, 295 ± 0.5 K.

III. Results and Discussion

A. Steady State Studies. Absorption and emission spectra of P4C in TBA−water solutions at TBA mole fractions 0.01, 0.04, 0.1, 0.6 and that in pure TBA are shown in Figure 1. These TBA mole fractions are chosen so that the effects of gradual change in H-bonding structure (from tetrahedral-like network at low concentration to zigzag chain at higher mole fractions) on the stabilization of the ground and excited states of a fluorescent probe are represented. As already mentioned, aqueous TBA solutions with low TBA mole fractions are characterized by aggregation of TBA molecules via interactions among hydrophobic tertiary butyl ($-CMe_3$, $Me = CH_3$) groups where the alcoholic hydroxyl (−OH) groups are incorporated into the water H-bonding cage that surrounds the TBA cluster. In concentrated TBA solution, both water and TBA molecules associate to form zigzag H-bonding chain structure similar to that in pure alcohol. Although the anomaly in thermodynamic properties of aqueous TBA solution is the maximum at 0.04 TBA mole fraction, 0.10 corresponds to the transition composition from the TBA−TBA intermolecular contact to the TBA−water molecular association.

One of the most interesting aspects of Figure 1 is that at low TBA mole fractions (up to ∼0.1), absorption spectrum of P4C

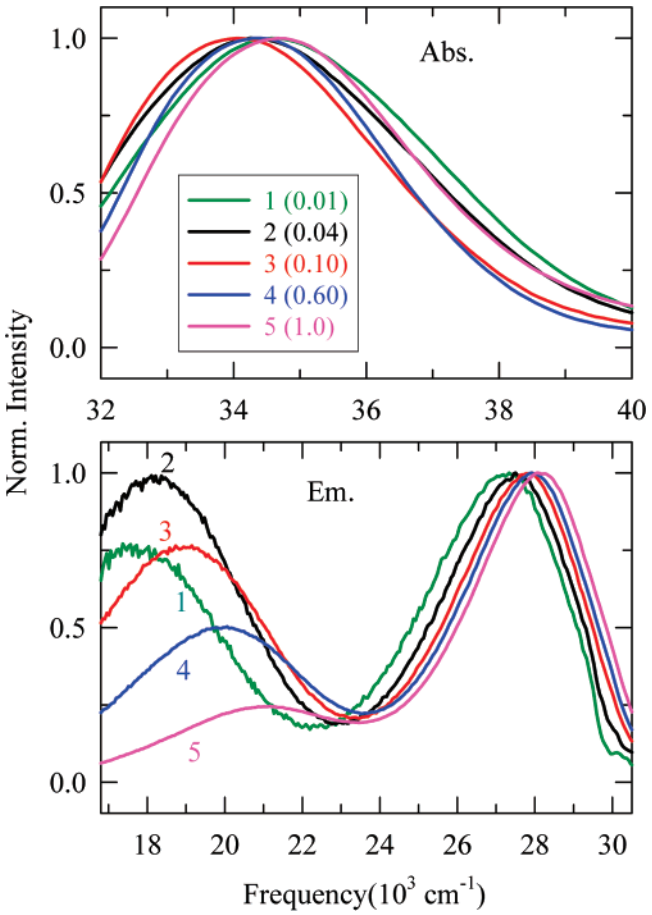

Figure 1. Absorption and emission spectra of 4-(1-azetidinyl)-benzonitrile (P4C) in different mole fractions of tertiary butyl alcohol of the mixture of water and tertiary butyl alcohol (TBA). The upper panel shows the absorption spectra and lower panel shows the emission spectra. The numbers in parentheses indicate the TBA mole fraction in the TBA−water mixtures. Note that the absorption spectra are presented in a relatively narrower frequency scale to enhance the separation between spectra.

shows red shift with the increase in TBA concentration, whereas emission spectrum shifts toward blue. At mole fractions higher than 0.1, both absorption and emission spectra show blue shift with TBA concentration as the average polarity of the medium decreases. The alcohol mole fraction dependence of absorption and emission spectra and their bandwidths (full width at half-maximum) have been studied in detail and are summarized in Figure 2 where the peak frequencies of absorption and emission bands (both LE and CT) and spectral widths are shown as a function of TBA mole fraction. Several interesting aspects are to be noted in this figure. First, the absorption spectrum shows a red shift with the increase in alcohol concentration up to TBA mole fraction ∼0.10 and then blue shifts upon further addition of TBA. Contrastingly, the emission spectrum exhibits a continuous blue shift with TBA mole fraction in a fashion that resembles the typical nonideality in average polarity of such alcohol−water mixtures. Note that for the entire range of TBA concentration, the total blue shift for the CT band is ∼2500 cm^{-1}, whereas it is ∼1000 cm^{-1} for the LE band. Because addition of TBA in water facilitates formation of TBA clusters and enhances the H-bonding between all species, the micro-heterogeneity and the related structural modifications will affect the spectral properties of a dissolved solute. The enhanced H-bonding structure at low TBA concentrations is further probed by a recent study on compressibility of TBA−water mixtures using the RISM theory[64] where realistic potentials have been used to represent both the species.[63−64] This theoretical study and comparisons with relevant experimental data have suggested that at low TBA concentration the cavity in the H-bonding network of water is occupied by the alkyl groups of the clustered TBA molecules, thereby reducing the compressibility of the solution.[64] Therefore, the reduced compressibility is an indicative of a more compact solvation environment surrounding the probe (P4C) molecule. This increased compactness due to the enhancement of local structure then naturally stabilizes the ground state energy level of the probe, leading to the observed red shift in the absorption spectrum. However, with further addition of TBA, tetrahedral-like network of H-bonding structure of water-rich solutions gradually converts to the chain-like alcohol structure at concentrated TBA solutions. Several studies[47−65] of TBA−water systems have revealed that such a structural transition occurs at TBA mole fraction ∼0.10, a value at which the absorption peak frequency of P4C in the present study also shows a turnaround. However, the question is then why emission frequency does not exhibit such a TBA mole fraction dependence? Simulation studies of TBA−water solutions have indicated that even though clusters of three or four TBA molecules are formed but undergo continual change on time scales of tens of picoseconds.[61] Because the stability times of these clusters (20−30 ps)[61] are many times smaller than the average lifetime of the excited state (>1 ns) of the probe, the solvent environment surrounding the photoexcited probe undergoes a large number of relatively rapid fluctuations. These environmental fluctuations average out the subtle structural modification in dilute aqueous solutions of TBA, allowing the solution polarity to primarily govern the emission transition energy.

Second interesting aspect of Figure 2 is the TBA mole fraction dependence of absorption and emission bandwidths of P4C. The absorption bandwidth (bottom-left panel) shows a sharp decrease with TBA mole fraction up to ∼0.10. However, the dependence of absorption bandwidth on TBA mole fraction is weaker in the range 0.10−1.0 and the total decrease in bandwidth in this range is only about 250 cm^{-1}, which is similar to frequency shift *versus* bandwidth behavior observed earlier with P4C in electrolyte solutions and also with a different solvation probe in neat solvents. The narrowing of absorption spectrum of P4C by ∼1000 cm^{-1} upon increasing the TBA concentration to ∼0.10 mole fraction is anomalously large and apparently contradicts the observations made in earlier studies.[69] As the spectral width in a binary mixture derives contributions from both the probe−solvent interaction strength and the heterogeneity in the surrounding solvent environment due to both density and concentration fluctuations, the narrowing of absorption spectrum may be regarded as a reflection of a novel interplay between the lowering of polarity and the loss of microscopic heterogeneity on each successive addition of TBA in water. The arguments given above may also be used to explain the narrowing of both the LE and CT emission bands between 0.10−1.0 TBA mole fractions. The blue shift with broadening in LE emission band and red shift with narrowing in the CT emission band have also been observed earlier for a nonreactive solvation probe coumarin 153 (C153) in pure solvents.[69] We mention here that for C153 in hexane−alcohol binary mixtures, the emission bandwidth is found to increase up to alcohol mole fraction ∼0.10 and then decreases with further addition of alcohol.[23] This has been explained in terms of heterogeneity of solution structure.[23] However, no information is available in this study regarding the correlation between the red shift of the absorption spectrum and the absorption bandwidth.

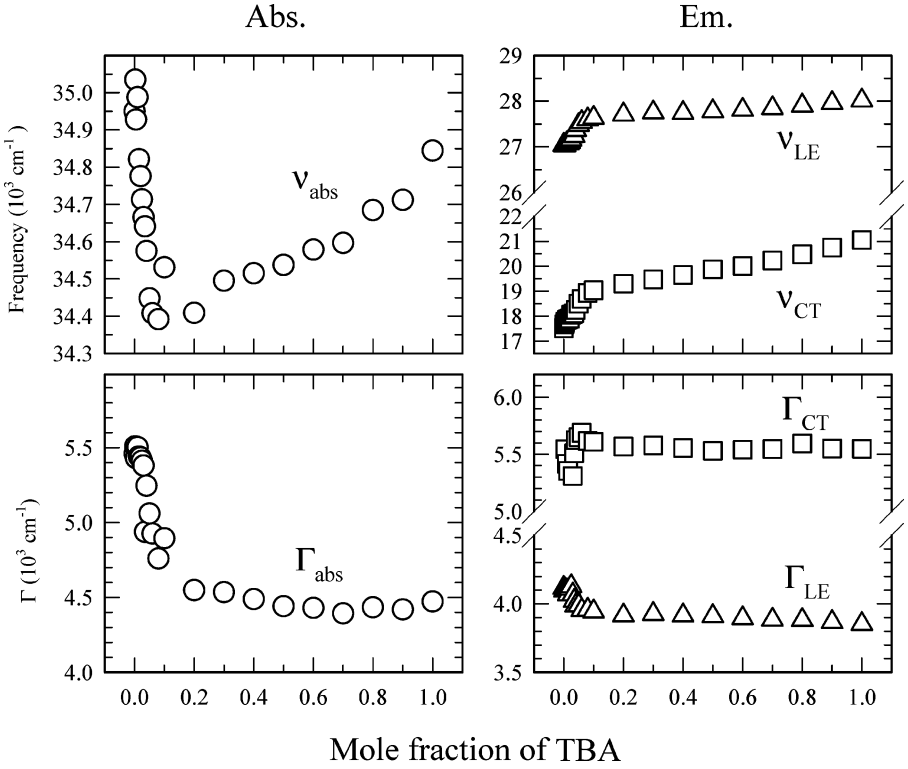

Figure 2. Mole fraction dependence of absorption (ν_{abs}) and emission (ν_{LE} and ν_{CT}) peak frequencies and line widths (full width at half-maxima, Γ) of the absorption spectra, LE bands, and CT bands of 4-(1-azetidinyl)benzonitrile (P4C) have been shown in a water and TBA mixture. The open circles (in the left panel) represent absorption and open triangles and squares (in the right panel) represent the parameters associated with LE and CT bands of P4C. LE and CT peak frequencies (ν_{LE} and ν_{CT}) have been obtained after deconvoluting the experimental emission spectra by broadening and shifting a reference spectrum with a Gaussian function (representing inhomogeneous solvent broadening). Γ_{LE} and Γ_{CT} are the full width at half-maxima of LE and CT bands obtained after deconvoluting the full experimental emission spectrum. The estimated uncertainty in frequencies and widths is $\pm$300 cm^{-1}.

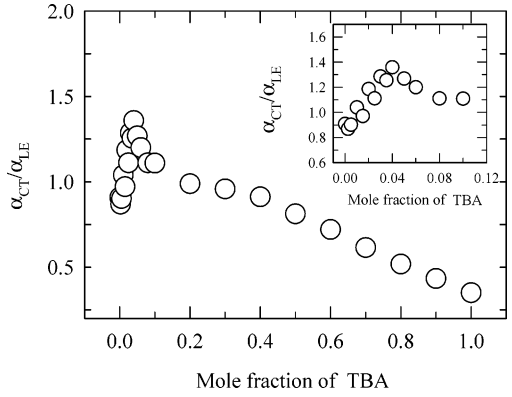

Figure 3. Mole fraction dependence of formation of CT population in the mixture of TBA and water has been shown in this figure. The ratio (α_{CT}/α_{LE}) between areas under the CT and LE bands are shown as a function of mole fraction of TBA. The inset shows α_{CT}/α_{LE} in the breaking region.

Figure 3 depicts the TBA mole fraction dependence of the ratio between areas under the CT and LE emission bands of P4C in TBA−water solution. Note the area ratio shows a nonmonotonic dependence on TBA concentration with a peak at TBA mole fraction ~0.04. This is the mole fraction of TBA where the maximum anomaly in thermodynamic properties as well as large increase in ultrasonic absorption[72−74] and light scattering[52−53] has been observed. The reasons for the anomalous increase in the area ratio (CT/LE) in dilute aqueous solutions of TBA can be understood by examining the LE and CT emission bandwidths of P4C. The alcohol mole fraction dependent bandwidths presented in Figure 2 indicate that although the LE emission band narrows down upon addition of TBA, the width of the CT emission band increases up to TBA mole fraction ~0.04 and then decreases. Therefore, the simultaneous broadening of the CT emission band with the narrowing of the LE band leads to the sharp increase of the area ratio (CT/LE) at ~0.04 TBA mole fraction. As the CT state is primarily of L_a character and therefore more polar than the LE state (L_b),[5] coupling of these states with the mole fraction dependent solution structure (environment) is likely to be different. This might be the reason for the observed difference in the mole fraction dependence of the LE and CT emission bandwidths.

We have measured quantum yield, radiative and nonradiative rates, and transition moments of P4C at different mole fractions of TBA in aqueous solution to investigate the effects of solution structure on these quantities. Quantum yield has been determined by using the following relation[5]

$$\Phi_S = \Phi_R\left(\frac{n_S}{n_R}\right)^2\left(\frac{I_S}{I_R}\right)\left(\frac{1-10^{-0.5A_R}}{1-10^{-0.5A_S}}\right) \quad (1)$$

Quinine sulfate dihydrate in 0.05M H_2SO_4 has been used as reference ($\Phi_R = 0.508$).[5] In eq 1, n_x represents refractive index of the reference solution (R) and sample (S), I the integrated emission intensity, and A the absorbance. Refractive indices of the TBA−water solutions at different mole fractions of TBA have been measured (296.15 ± 1 K) and summarized in Table 1. Quantum yields (net) of P4C determined at various mole fractions of TBA in aqueous solutions are shown in the upper panel of Figure 4. As expected, the mole fraction dependence of quantum yield is a nonideal one and similar to that of LE and CT emission frequencies. Similar alcohol mole fraction dependence is also found for the quantum yields for the

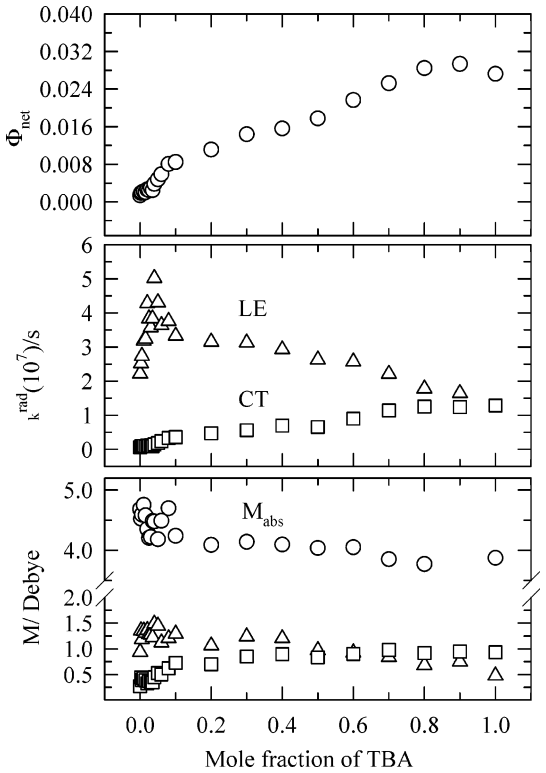

Figure 4. Mole fraction dependence of quantum yield (Φ_{net}), radiative rate (k^{rad}), absorption transition moment, and emission (LE and CT) transition moments for P4C in a water and TBA mixture have been shown in this figure. Open circles in the upper panel show the net quantum yield of P4C in the mixture. Open triangles and open squares in the middle panel indicate the radiative rate of P4C associated with LE and CT bands, respectively. Open circles, open triangles, and open squares in the lower panel indicate absorption, LE, and CT transition moments, respectively.

TABLE 1: Refractive Indices and Nonradiative Rates Associated with LE Emission Band of P4C in Water−TBA Mixtures at Different TBA Mole Fractions

TBA mole fraction	n_s	$10^9 k_{LE}^{nr}$/s
0	1.331	31.40
0.0025	1.333	27.21
0.005	1.333	27.31
0.01	1.335	28.48
0.015	1.336	30.85
0.02	1.338	30.20
0.025	1.340	27.85
0.03	1.341	21.65
0.035	1.344	27.12
0.04	1.345	22.65
0.05	1.346	15.78
0.06	1.350	11.13
0.08	1.355	8.71
0.1	1.357	7.50
0.2	1.368	5.63
0.3	1.373	4.80
0.4	1.376	4.75
0.5	1.379	3.41
0.6	1.380	2.82
0.7	1.381	2.27
0.8	1.381	1.81
0.9	1.381	1.46
1	1.382	1.16

individual LE and CT bands (not shown here). Note that the quantum yield of P4C in pure TBA is very close to that in pure methanol ($\Phi_{net} = 0.016$).[5]

The following relation has been used to determine the radiative rate for the LE band:[5] $k_{LE}^{rad} = \phi_{LE}/\langle\tau_{LE}\rangle$, where the average LE lifetime ($\langle\tau_{LE}\rangle$) has been calculated by using the relation [5]$\langle\tau_{LE}\rangle = \sum_i a_i\tau_i/\sum_i a_i$. The amplitudes ($a_i$) and time constants ($\tau_i$) are obtained by fitting the relevant LE emission decays. The nonradiative rate for LE (k_{LE}^{nr}) is then calculated by using the relation,[5] $k_{LE}^{nr} = (1 - \phi_{LE})/\langle\tau_{LE}\rangle$. For CT, the radiative rate is obtained as follows:[5] $k_{CT}^{rad} = \phi_{CT}k_{dec}(1 + K_{eq}^{-1})$, where the average excited state population decay constant, (k_{dec}), as shown in Scheme 3 of ref 5, is determined from the net rate constants k_{LE} and k_{CT} using $k_{dec} = (k_{LE} + k_{CT})/2$, and assuming rapid equilibrium between LE and CT states.[5] The calculated radiative rates for the LE and CT emission bands of P4C at different mole fractions of TBA in aqueous solution of TBA are shown in the middle panel of Figure 4. The corresponding nonradiative rates for the LE emission band are summarized in Table 1. The parameters necessary for the calculations of $\langle\tau_{LE}\rangle$ and k_{CT} are obtained from the decay fits (shown later in Figure 6). The error bar for these radiative and nonradiative rates is ±25% of the values reported here. It is interesting to note that k_{LE}^{rad} shows a peak at TBA mole fraction ~0.04, whereas k_{CT}^{rad} exhibits a typical nonideal TBA mole fraction dependence. The fit parameters shown later in Figure 6 indicate that there would be a minimum in $\langle\tau_{LE}\rangle$ at TBA mole fraction ~0.04, which is responsible for the observed peak in k_{LE}^{rad}.

Because the enhancement of solution structure at very low concentration of TBA significantly affects the absorption peak frequencies of the probe molecule, the absorption transition moment is also expected to show the effects of such structural modifications. The following relation[5,18] has been used to calculate the net absorption transition moment of the composite absorption band ($S_0 \rightarrow L_a + S_0 \rightarrow L_b$)

$$M_{abs}/D = 9.584 \times 10^{-2}\left[\frac{1}{n_s}\int_{abs}(\epsilon(\nu)/\mathrm{M}^{-1}\,\mathrm{cm}^{-1})\,\frac{d\nu}{\nu}\right]^{1/2} \quad (2)$$

where $\epsilon(\nu)$ is the molar decadic extinction coefficient. The net absorption transition moment thus obtained for P4C in water−TBA mixtures are shown as a function of TBA mole fraction in the bottom panel of Figure 4. The maximum error bar associated with this calculation is ±15% . The data in this figure (Figure 4) seem to suggest that the TBA induced enhancement of the H-bonding structure have small but non-negligible effects on the net absorption transition moment of P4C. However, once the tetrahedral-like H-bonding network structure of water is disrupted and chain-like structure of alcohol appears upon further addition of TBA, the net absorption transition moment becomes almost insensitive to the TBA mole fraction beyond ~0.10. The near insensitivity of the net absorption transition moment of P4C on the average polarity of the medium has also been observed earlier in neat solvents[5] and also in electrolyte solutions.[18] All these observations probably indicate that the solution structure rather than the polarity of the medium dictates the absorption transition moment in solution phase.

To investigate the effects of microheterogeneity and structural transition, the TBA mole fraction dependence of emission transition moment for P4C in water−TBA solution has also been studied. Emission transition moments (M_x) for P4C have been determined from the radiative rate data by using the following relation[5,18]

$$M_x/D = 1785.7\left(\frac{k_x^{rad}/\mathrm{s}^{-1}}{n_s^3(\tilde{\nu}_x^3/\mathrm{cm}^{-3})}\right)^{1/2} \quad (3)$$

where $\tilde{\nu}_x^3 = \int F_x(\nu)\, d\nu / \int F_x(\nu)\nu^{-3}\, d\nu$, with $F_x(\nu)$ denoting the fluorescence spectrum of species x = LE or CT. The results are also shown in the bottom panel of Figure 4. It is interesting to note that the emission transition moment for the LE band does not show a sharp rise upon increasing the alcohol concentration in the water rich region of the aqueous solution, even though the LE radiative rate (k_{LE}^{rad}) shows a peak at TBA mole fraction ~0.04. However, both the LE and CT emission transition moments exhibit near insensitivity to alcohol concentration beyond TBA mole fraction ~0.10. The nonradiative rates for the LE band at different TBA mole fractions have also been calculated and are summarized in Table 1. Note that the nonradiative rate for LE (k_{LE}^{nr}) is very large in very dilute solutions of TBA, which becomes comparable to that for P4C in methnol at TBA mole fraction ~0.10. It is probably the H-bonding network of water that facilitates the nonradiative relaxation processes and hence the nonradiative rates are very large for LE in the aqueous solution at TBA mole fraction <0.05. This observation again suggests an appreciable role of solution structure in determining the nonradiative rate for an emission band.

B. Time-Resolved Fluorescence Emission Studies. Time-resolved emission decay measurements have been performed with P4C in water−TBA mixtures at 23 different TBA mole fractions to study the effects of TBA-induced structural transition and microscopic heterogeneity of water−TBA solutions on the rate of LE → CT conversion reaction in P4C. As already mentioned in the Introduction, emission decays of P4C in water−TBA solution are biexponential with time at all TBA mole fractions. This is rather interesting because in water−TBA mixtures where microscopic heterogeneity governs the solution structure, a stretched exponential[75] rather than a simple biexponential function is expected to properly describe the decay kinetics. The fact that a time dependent biexponential function can sufficiently describe the decay kinetics of P4C in water−TBA mixtures is a reflection of rapid fluctuations in the immediate environment of the photoexcited P4C due to relatively faster lifetime of the TBA clusters. It may also be due to the fact that because a broader time resolution (fwhm of the IRF) is employed in this study, missing of faster components inhibits the detection of the subtle variation in the faster time scales. Representative biexponential fits to the emission decays collected at peak wavelengths of LE and CT bands of P4C at 0.60 mole fraction of TBA are shown in Figure 5 where fit parameters are also listed. Clearly, both the LE and CT emission decays are biexponential as the residuals do not contain any nonrandom pattern[76] and values for the "*goodness of fit parameter*" (χ^2) are close to 1.

Figure 5 also demonstrates that when the fits are carried out without any constraints, time constants describing the CT emission decay are very similar to those required to fit the corresponding LE decays. As shown in the lower panel of Figure 5, "free" fitting of CT emission decay at 0.60 TBA mole fraction produces time constants 220 ps (rise time) and 2150 ps with $\chi^2 = 1.08$. The time constant associated with the rise (rise time) is thus very similar to the fast time constant (decay time, 201 ps) of the LE decay, indicating that these time constants are essentially associated with the average reaction rate[5] for the LE → CT conversion reaction of P4C. Note here that fixing of the rise time to the fast decay time constant of LE emission decay (201 ps) or addition of a third exponential did not produce a better fit. We would see soon that similar behavior has been observed at all TBA mole fractions. It is therefore interesting to note that self-association of TBA molecules in water−TBA mixtures has not induced any deviation from the biexponential kinetics observed earlier for P4C in neat solvents[5] and electrolyte solutions.[19] Therefore, the biexponential behavior of the decay kinetics for P4C in water−TBA mixtures also conform to the classical two state reversible reaction mechanism as described by Maroncelli and co-workers in ref 5.

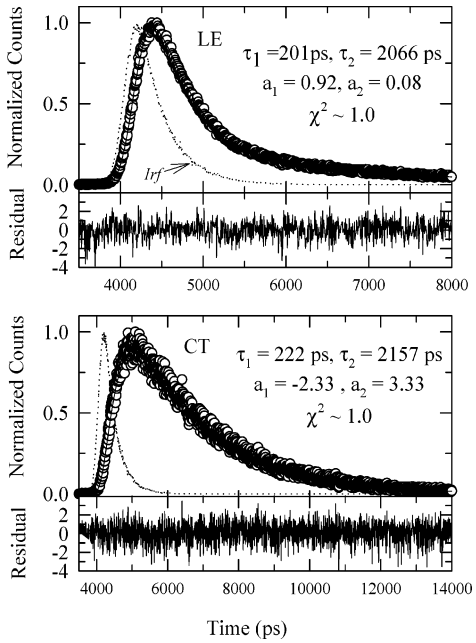

Figure 5. Representative LE emission decay (upper panel) and CT emission decay (lower panel) of P4C in the mixture of water and TBA at the mole fraction of 0.6 of TBA have been shown in this figure. The data are represented by the circles, and the fit through the data is by the solid line. The instrument response function is shown by the broken line. The fit (biexponential) results are also provided in the upper panel as well as in the lower panel. The LE peak count is ~3000 and the CT peak count is ~1000. Residuals are shown at the bottom of each panel (±4 full scale).

The average reaction time can be obtained from the collected LE emission decay from the following relation:[5]

$$\tau_{rxn}^{avg} = \frac{\sum_{i=1}^{n-1} a_i \tau_i}{\sum_{i=1}^{n-1} a_i} \qquad (4)$$

where a_i and τ_i are the fractional amplitudes and time constants observed in *n*-exponential fit. Note that in the present study the fast time constant is simply the average reaction time as the decays are all biexponential with time. The average reaction time (τ_{rxn}^{avg}) for P4C in water−TBA solutions are shown as a function of TBA mole fraction in the upper panel of Figure 6. The TBA mole fraction dependence of the reaction time therefore clearly reflects the nonideality of the water−TBA binary mixture. The reaction time in pure TBA is ~300 ps which is similar to that in pure 1-pentanol.[5] As the static dielectric constants (ϵ_0) of TBA and 1-pentanol are 12.5 and 13.9, respectively,[69] the similarity in reaction time probably indicates that the average polarity of the medium largely governs the LE → CT conversion reaction in P4C. The fact that the average reaction time is ~6 times faster in extremely dilute TBA solution than that in pure TBA provides further support to this conclusion as earlier studies[77,78] with DMABN in butyronitrile−octane and butanol−hexadecane mixtures showed the rate being proportional to the polarity parameter $E_T(30)$.

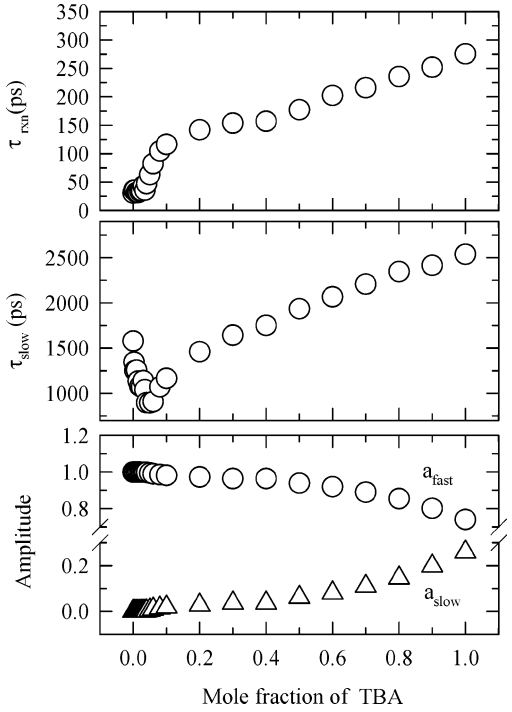

Figure 6. Mole fraction dependence of the reaction time ($\tau_{rxn} = \tau_{fast}$), time constant associated with the slow component of the biexponential emission decay (τ_{slow}) and that of amplitudes (a_{fast} and a_{slow}) associated with the LE → CT conversion reaction of P4C in aqueous solutions of TBA. The upper and middle panels show respectively the variation of τ_{rxn} and τ_{slow} with TBA mole fraction, and the lower panel shows the same for the amplitudes obtained from biexponential fits to the collected emission decays.

As the H-bonding network structure is believed to be strengthened upon addition of TBA in very dilute aqueous solutions, the increased "compactness" (as reflected in the lowering of isothermal compressibility)[64] of the solvation environment may affect the rate of LE → CT conversion reaction. The effects of such structural transition on the reaction rate should be reflected in the alcohol concentration dependence of τ_{rxn}^{avg} in the water-rich region of water−TBA mixtures. However, for the reasons already stated, the subtle variation in τ_{rxn}^{avg} with TBA concentration in the very dilute TBA solution could not be captured successfully. However, a closer look at these data seems to suggest a broad minimum in τ_{rxn}^{avg} at TBA mole fraction <0.05. Note that the values of τ_{rxn}^{avg} at these TBA mole fractions are much smaller than the effective resolution of our decay analysis method and are therefore likely to be associated with large uncertainties. However, these data are reproducible and the variation with alcohol concentration appears to be systematic. Therefore, the broad minimum at low TBA mole fraction may arise due to the TBA-induced compactness of the network structure which favors the formation of CT upon photoexcitation of P4C molecule. Note that steady state results presented in Figure 3 also bear the signature of such structural enhancement. Therefore, further studies with better time resolution are required to unravel the effects of structure enhancement on reaction rate in the very dilute aqueous solutions of TBA.

The effects of enhanced solution structure are clearly observed when the time constant associated with the slower component of the emission decay is plotted as a function of TBA mole fraction. This is shown in the middle panel of Figure 6. Note the presence of a minimum in τ_{slow} at TBA mole fraction ∼0.04. The bottom panel of Figure 6 depicts the amplitudes as a function of TBA concentration obtained from the biexponential fits to the LE emission decays. The TBA mole fraction dependence of the amplitudes indicate that the LE → CT conversion reaction is increasingly disfavored as the polarity of the medium is decreased with successive addition of TBA. Also, at the water-rich region, the overwhelming domination of the fast component (a_{fast}) over the other one (a_{slow}) suggests that the reaction is highly favorable due to the large value of change in reaction free energy ($-\Delta G_r \propto \ln[a_{fast}/a_{slow}]$).[5] Note here that even though the magnitude of a_{slow} is very small at TBA mole fractions <0.10, neglect of this does not produce a good fit (as indicated by χ^2 and nonrandom pattern of the residual).

IV. Conclusion

Let us first summarize the main results of the paper. Although the absorption spectrum of P4C shows a red shift with alcohol concentration in the TBA mole fraction regime 0.0−0.10 and then blue shifts with further addition of TBA in the aqueous solution, the emission spectrum exhibits a continuous blue shift in the entire range of alcohol concentration. The nonideality in solution polarity with alcohol mole fraction seems to be the main guiding factor for the emission shifts, whereas the absorption characteristics pick up also the effects of structural enhancement at very low TBA concentration. The relatively faster lifetime of the TBA clusters probably contributes to the "homogenization" of the otherwise microscopically heterogeneous solution structure, and hence the steady state fluorescence emission does not show any characteristics of the solution inhomogeneity.

The spectral broadening and shifts for P4C with TBA mole fraction are found to be different from those in neat solvents and also in electrolyte solutions. The full width at half-maximum (FWHM) of absorption spectrum is found to narrow with red shift in the range 0.0−0.10 mole fraction of TBA, which is opposite in direction to that found in systems where simply the average polarity is changed.[5,18,69] The CT emission band also shows spectral broadening with a blue shift in the same range (0.0−0.10) of TBA mole fraction, which is contrary to the expectation based on earlier observations.[5,18,69] At TBA mole fraction higher than 0.10, the narrowing and shifts of the absorption and CT emission bands correlate well with the earlier results.[19,69] The LE emission band, however, narrows as it shifts toward higher energy upon addition of TBA and shows a nonideal alcohol concentration dependence. The opposite alcohol mole fraction dependence of the LE and CT emission bandwidths in the very dilute aqueous solutions of TBA is mainly responsible for the sharp rise in the CT/LE area ratio at TBA mole fraction ∼0.04.

Nonideal alcohol mole fraction dependence is also found for quantum yield and transition moments for LE and CT emission bands. Although the radiative rate associated with the LE emission band shows a small increase with TBA concentration in the very dilute solution, the CT radiative rate exhibits nonideal TBA mole fraction dependence. The absorption transition moment is also found to show a small increase in the TBA mole fraction range 0.0−0.10. It would be worth noting that the nonmonotonic dependence of quantum yield on solvent polarity has been observed earlier[79] with *N*,*N*-(dimethylamino)benzonitrile (DMABN) molecule in binary mixtures of n-octane and propionitrile. The observed nonmonotonic dependence of TICT emission on propionitrile concentration has been explained in terms of a competition between the formation of the TICT state and the decay through nonradiative pathways. Such an analysis

might be attempted to learn more about the competing processes for this ring compound and its analogues in alcohol−water binary mixtures.

The time dependent decay of the emission intensity is found to be biexponential for all TBA mole fractions even though microscopic heterogeneity is one of the characteristics of water−TBA solutions. This demonstrates that the decay kinetics of P4C in water−TBA mixtures also conform to the two state model as envisaged earlier.[5,19] The time constant associated with the slower component of the biexponential decay shows the effects of TBA-induced structural enhancement at very dilute solutions of TBA. However, at higher alcohol concentration, τ_{slow} shows the expected nonideal TBA mole fraction dependence.

We mention here that initial studies[80] by using a well-known solvation probe (C153) in water−TBA mixtures also reveal the similar steady state characteristics as have been found for P4C. When a better time resolution (FWHM ∼75 ps) is used to study the time dependent rotational anisotropy ($r(t)$) of C153 in this mixture, $r(t)$ is found to be biexponential at all TBA concentrations. Moreover, studies with P4C in water−ethanol, water−ethylene glycol, and DMSO−acetonitrile mixtures also indicate the biexponential decay kinetics.[81] Because slow solvation dynamics due to preferential solvation in these binary mixtures is likely to play an important role in determining the rate of TICT reaction, study of solvation dynamics in these media is required to explore the dynamic solvent control of the reaction rates.[23−35,82,83] Therefore, further studies with different TICT molecules using a better time resolution is required where effects on the TICT reaction of the novel interplay between the hydrophobic and H-bonding interactions governing the structure and dynamics in binary mixtures can be better understood. Another interesting study would be the temperature dependence of the TICT reaction in the 0.04 mole fraction TBA−water solution. This system has recently[84] been shown to display significant meso-scale molecular aggregation and deaggregation as the temperature of the solvent is increased from room temperature to ∼383 K. It would consequently be interesting to see how the TICT process varies in the system as the structural correlations in the solvent are varied over nanometer length scales.

Acknowledgment. It is a pleasure to thank Professors B. Bagchi and M. Maroncelli for constant encouragement, kind assistance, and support. Encouragement received from Professor A. K. Raychaudhuri is gratefully acknowledged. We thank an anonymous reviewer for pointing out several important references. Financial supports from the Department of Science and Technology (DST), India and Council of Scientific and Industrial Research (CSIR), India, are gratefully acknowledged. T.P. acknowledges the University Grants Commission (UGC), India, for a research fellowship.

References and Notes

(1) Grabowski, Z. R.; Rotkiewicz, K.; Rettig, W. *Chem. Rev.* **2003**, *103*, 3899.
(2) Lippert, E.; Rettig, W.; Bonacic-Koutecky, V.; Heisel, F.; Mieche, J. A. *Adv. Chem. Phys.* **1987**, *68*, 1.
(3) Zachariasse, K. A.; Druzhinin, S. I.; Bosch, W.; Machinek, R. *J. Am. Chem. Soc.* **2004**, *126*, 1705.
(4) Techert, S.; Zachariasse, K. A. *J. Am. Chem. Soc.* **2004**, *126*, 5593.
(5) Dahl, K.; Biswas, R.; Ito, N.; Maroncelli, M. *J. Phys. Chem. B* **2005**, *109*, 1563.
(6) Zachariasse, K. A. *Chem. Phys. Lett.* **2000**, *320*, 8.
(7) Zgierski, M. Z.; Lim, E. C. *Chem. Phys. Lett.* **2004**, *393*, 143.
(8) Rettig, W. *J. Luminesc.* **1980**, *26*, 21; *J. Phys. Chem.* **1982**, *86*, 1970.
(9) Rettig, W.; Gleiter, R. *J. Phys. Chem.* **1985**, *89*, 4674.
(10) Rettig, W.; Wermuth, G. *J. Photochem.* **1985**, *28*, 351. Al-Hassan, K. A.; Rettig, W. *Chem. Phys. Lett.* **1986**, *126*, 273. LaFemina, J. P.; Duke, C. B.; Rettig, W. *Chem. Phys.* **1990**, *87*, 2151. Braun, D.; Rettig, W. *Chem. Phys.* **1994**, *180*, 231; *Chem. Phys. Lett.* **1997**, *268*, 110.
(11) Rettig, W. *Ber. Bunsen-Ges. Phys. Chem.* **1991**, *95*, 259.
(12) Yatsuhashi, T.; Trushin, S. A.; Fuss, W.; Rettig, W.; Schmid, W. E.; Zilberg, S. *Chem. Phys.* **2004**, *296*, 1.
(13) Zachariasse, K. A.; Grobys, M.; von der Haar, T.; Hebecker, A.; Il'ichev, Y. V.; Jiang, Y.-B.; Morawski, O.; Kuhnle, W. *J. Photochem. Photobiol. A* **1996**, *102*, 59.
(14) Rettig, W.; Zeitz, B. *Chem. Phys. Lett.* **2000**, *317*, 187.
(15) Parusel, A. B. J. *Chem. Phys. Lett.* **2001**, *340*, 531.
(16) Wang, Y.; Eisenthal, K. B. *J. Chem. Phys.* **1982**, *77*, 6076.
(17) Wang, Y.; McAullffe, M.; Novak, F.; Eisenthal, K. B. *J. Phys. Chem.* **1981**, *85*, 3736.
(18) Pradhan, T.; Biswas, R. *J. Phys. Chem. A* **2007**, *111*, 11514.
(19) Pradhan, T.; Biswas, R. *J. Phys. Chem. A* **2007**, *111*, 11524.
(20) Zwan, van der G.; Hynes, J. T. *Chem. Phys.* **1991**, *152*, 169.
(21) Hynes, J. T. *Charge-Transfer Reactions and Solvation Dynamics In Ultrafast Dynamics of Chemical Systems*; Simon, J. D., Ed.; Kluwer: Dodrecht, 1994; p 345.
(22) Bagchi, B.; Biswas, R. *Adv. Chem. Phys.* **1999**, *109*, 207.
(23) Cichos, F.; Willert, A.; Rempel, U.; von Borczyskowski, C. J. *Phys. Chem. A* **1997**, *101*, 8179.
(24) Cichos, P.; Brown, R.; Rempel, U.; von Borczyskowski, C. *J. Phys. Chem. A* **1999**, *103*, 2506.
(25) Luther, B. M.; Kimmel, J. R.; Levinger, N. E. *J. Chem. Phys.* **2002**, *116*, 3370.
(26) Chandra, A.; Bagchi, B. *J. Chem. Phys.* **1991**, *94*, 8367.
(27) Chandra, A. *Chem. Phys. Lett.* **1995**, *235*, 133.
(28) Jarzeba, W.; Walker, G. C.; Johnson, A. E.; Barbara, P. F. *Chem. Phys.* **1991**, *152*, 57.
(29) Gardecki, J. A.; Maroncelli, M. *Chem. Phys. Lett.* **1999**, *301*, 571.
(30) Ladanyi, B. M.; Skaf, M. S. *J. Phys. Chem. A* **1996**, *100*, 18258.
(31) Laria, D.; Skaf, M. S. *J. Chem. Phys.* **1999**, *111*, 300.
(32) Day, T. J. F.; Patey, G. N. *J. Chem. Phys.* **1997**, *106*, 2782.
(33) Day, T. J. F.; Patey, G. N. *J. Chem. Phys.* **1999**, *110*, 10937.
(34) Yoshimori, A.; Day, T. J. F.; Patey, G. N. *J. Chem. Phys.* **1998**, *108*, 6378.
(35) Yoshimori, A.; Day, T. J. F.; Patey, G. N. *J. Chem. Phys.* **1998**, *109*, 3222.
(36) Bhattacharyya, K. *Acc. Chem. Res.* **2003**, *36*, 95 and references therein.
(37) Huppert, D.; Ittah, V.; Kosower, M. *Chem. Phys. Lett.* **1989**, *159*, 267.
(38) Bart, E.; Huppert, D. *Chem. Phys. Lett.* **1992**, *195*, 37.
(39) Ittah, V.; Huppert, D. *Chem. Phys. Lett.* **1990**, *173*, 496.
(40) Chapman, C. F.; Maroncelli, M. *J. Phys. Chem.* **1991**, *95*, 9095.
(41) Franks, F.; Ives, D. J. G. *Q. Rev. Chem. Soc.* **1966**, *20*, 1.
(42) Zeidler, M. D. *In Water, a Comprehensive Treatise*; Franks, F., Ed.; Plenum: New York, 1973; Vol. 2, p 529.
(43) Arnett, E. M.; McKlevey, D. R. *J. Am. Chem. Soc.* **1966**, *88*, 5031.
(44) Arnett, E. M.; McKlevey, D. R. *J. Am. Chem. Soc.* **1965**, *87*, 1393.
(45) Yamaguchi, T. *Pure Appl. Chem.* **1999**, *71*, 1741 and references therein.
(46) Cinelli, S.; Onori, G.; Santucci, A. *Colloids Surf. A.* **1999**, *160*, 3 and references therein.
(47) Bowron, D. T.; Finney, J. L.; Soper, A. K. *J. Phys. Chem. B* **1998**, *102*, 3551.
(48) Bowron, D. T.; Moreno, S. D. *J. Chem. Phys.* **2002**, *117*, 3753.
(49) Bowron, D. T.; Moreno, S. D. *J. Phys. Chem. B* **2005**, *109*, 16210.
(50) Dixit, S.; Crain, J.; Poon, W. C. K.; Finney, J. L.; Soper, A. K. *Nature* **2002**, *416*, 829.
(51) Soper, A. K.; Finney, J. L. *Phys. Rev. Lett.* **1993**, *71*, 4346.
(52) Iwasaki, K.; Fujiyama, T. *J. Phys. Chem.* **1979**, *83*, 463; **1977**, *81*, 1908.
(53) Euliss, G. W.; Sorensen, C. M.; *J. Chem. Phys.* **1984**, *80*, 4767.
(54) Nishikawa, K.; Kodera, Y.; Iijima, T. *J. Phys. Chem.* **1987**, *91*, 3694.
(55) Nishikawa, K.; Iijima, T. *J. Phys. Chem.* **1993**, *97*, 10824.
(56) Koga, Y. *Chem. Phys. Lett.* **1984**, *111*, 176.
(57) Murthy, S. S. N. *J. Phys. Chem. A* **1999**, *103*, 7927.
(58) Sato, T.; Buchner, R. *J. Chem. Phys.* **2003**, *119*, 10789.
(59) Yoshida, K.; Yamaguchi, T. *Z. Naturforsch. A* **2001**, *56*, 529.
(60) Wojtkow, D.; Czarnecki, M. *J. Phys. Chem. A* **2005**, *109*, 8218.
(61) Kusalik, P. G.; Lyubartsev, A. P.; Bergman, D. L.; Laaksonen, A. *J. Phys. Chem. B* **2000**, *104*, 9533.
(62) Nakanishi, K.; Ikari, K.; Okazaki, S.; Touhara, H. *J. Chem. Phys.* **1984**, *80*, 1656.
(63) Yoshida, K.; Yamaguchi, T.; Kovalenko, A.; Hirata, F. *J. Phys. Chem. B* **2002**, *106*, 5042.
(64) Omelyan, I.; Kovalenko, A.; Hirata, F. *J. Theo. Comput. Chem.* **2003**, *2*, 193.

(65) Perera, A.; Sokolic, F.; Almasy, L.; Koga, Y. *J. Chem. Phys.* **2006**, *124*, 124515.
(66) Kohler, G.; Rechthaler, K.; Rotkiewicz, K.; Rettig, W. *Chem. Phys.* **1996**, *207*, 85.
(67) Meech, S. R.; Phillips, *Chem. Phys. Lett.* **1985**, *116*, 262.
(68) Weisenborn, P. C. M.; Varma, C. A. G. O.; De Haas, M. P.; Warman, J. M. *Chem. Phys. Lett.* **1986**, *129*, 562.
(69) Horng, M. L.; Gardecki, J. A.; Papazyan, A.; Maroncelli, M. *J. Phys. Chem. B* **1995**, *99*, 17311.
(70) Lewis, J. E.; Biswas, R.; Robinson, A. G.; Maroncelli, M. *J. Phys. Chem. B* **2001**, *105*, 3306.
(71) Biswas, R.; Lewis, J. E.; Maroncelli, M. *Chem. Phys. Lett.* **1999**, *310*, 485.
(72) Brai, M.; Kaatze, U. *J. Phys. Chem.* **1992**, *90*, 8946.
(73) Kaatze, U.; Pottel, R.; Schmidt, P. *J. Phys. Chem.* **1988**, *92*, 3669; **1989**, *93*, 5623.
(74) Kaatze, U.; Menzel, K.; Pottel, R. *J. Phys. Chem.* **1991**, *95*, 324.
(75) Arzhantsev, S.; Jin, H.; Ito, N.; Maroncelli, M. *Chem. Phys. Lett.* **2005**, *417*, 524.
(76) Bevington, P. R. *Data Reduction and Error Analysis for the Physical Sciences*; McGraw-Hill: New York, 1969.
(77) Hicks, J.; Vandersall, M.; Babarogic, Z.; Eisenthal, K. B. *Chem. Phys. Lett.* **1985**, *116*, 18.
(78) Hicks, J. M.; Vandersall, M. T.; Sitzmann, E. V.; Eisenthal, K. B. *Chem. Phys. Lett.* **1987**, *135*, 413.
(79) Nag, A.; Kundu, T.; Bhattacharyya, K. *Chem. Phys. Lett.* **1989**, *160*, 257.
(80) Pradhan, T.; Ghoshal, P.; Biswas, R. Unpublished results.
(81) Pradhan, T.; Ghoshal, P.; Biswas, R. Unpublished results.
(82) Mukherjee, S.; Sahu, K.; Roy, D.; Mondal, S. K.; Bhattacharyya, K. *Chem. Phys. Lett.* **2004**, *384*, 128.
(83) Molotsky, T.; Huppert, D. *J. Phys. Chem. A.* **2004**, *107*, 8449.
(84) Bowron, D. T.; Finney, J. L. *J. Phys. Chem. B* **2007**, *111*, 9838.